
CATALYSIS IN CHEMICAL AND PETROCHEMICAL INDUSTRY

Dehydrogenation of Methanol over Copper-Containing Catalysts

T. P. Minyukova^{a,*}, A. V. Khasin^{a,**}, A. A. Khassin^{a,b,***}, N. V. Shtertser^{a,b,****},
I. I. Simentsova^{a,*****}, and T. M. Yurieva^{a,*****}

^a*Boreshkov Institute of Catalysis, Siberian Branch, Russian Academy of Sciences, Novosibirsk, 630090 Russia*

^b*Novosibirsk State University, Novosibirsk, 630090 Russia*

**e-mail: min@catalysis.ru*

***e-mail: khasin@catalysis.ru*

****e-mail: khassinaa@mail.ru*

*****e-mail: nat@catalysis.ru*

******e-mail: sii@catalysis.ru*

******e-mail: yurieva@catalysis.ru*

Received March 4, 2016

Abstract—A comparative study of copper-containing catalysts with different chemical and phase compositions is performed to determine conditions for the implementation of the vapor phase and highly selective dehydrogenation of methanol to methyl formate or syngas. A thermodynamic analysis of the reaction is also performed. It is shown that Cu⁰ nanoparticles formed in the course of reductive activation reveal different selectivities with respect to the formation of methyl formate from methanol or its dehydrogenation with formation of syngas. By correctly selecting the catalyst composition and process conditions, high (90–100%) selectivity with respect to either methyl formate or syngas can be attained. Catalysts based on Cu–Zn hydrosilicate of the zincsilite type and on CuAlZn aurichalcite are highly selective in the process of methyl formate formation. An estimation based on experimental data shows that the productivity of Cu/SiO₂ catalyst, the one most effective in dehydrogenation to syngas, is as high as 20 m³/h of syngas at a methanol vapor pressure of 1 atm, a temperature of 200°C, and a contact time of 0.5 s.

Keywords: methanol dehydrogenation, methyl formate, syngas, partial equilibrium

DOI: 10.1134/S2070050416040073

INTRODUCTION

Investigating the reaction of catalytic dehydrogenation of methanol over copper-containing catalysts is of practical importance because the resulting methyl formate (MF) (which is anhydrous) is an initial reagent for the synthesis of numerous chemical products, e.g., DMFA, formamide, and formic and acetic acids [1]. The complete dehydrogenation of methanol into CO and H₂ is one of the methods for the laboratory scale production of syngas. Such studies are of prime interest in the theory of catalytic synthesis based on CO and H₂.

The results from numerous studies on methanol dehydrogenation over copper-containing catalysts, including Cu/SiO₂ [2–6], CuLaTi- and CuLaMn-oxide catalysts with structures of the perovskite type [7], Cu/ZnO [8], and Cu/CeO₂ [9], Cu/Cr₂O₃ [10], Cu/Al₂O₃ [11] and copper-containing catalyst for the synthesis of methanol [12, 13] have been published over the last three decades. These studies showed that the copper-containing catalysts were active in the reaction of methanol dehydrogenation only after reductive activation in a hydrogen atmosphere. The

data published in these works were obtained using catalysts of different natures, often prepared under conditions that were difficult to reproduce. Catalytic measurements were performed under conditions that were not comparable, and their activity was characterized by different indicators. It was therefore difficult to establish relationships between the catalytic properties, compositions, and structures of catalyst precursors. Establishing such relationships offers the opportunity to regulate the catalytic properties of oxide catalysts, including the reaction of methanol dehydrogenation, which proceeds in a reductive environment.

In this work, we discuss the results from comparative investigations of the catalytic properties of catalysts of the methanol dehydrogenation reaction that have copper-containing precursors with different compositions and structures:

- copper hydrosilicate with chrysocolla structure (Cu–Si);
- copper-zinc hydrosilicate with zincsilite structure (Cu–Zn–Si);

Table 1. Chemical and phase composition, according to XRD data and the specific surface areas of the calcined samples

Sample	Composition, at %					T_{calc} , °C	Phase compositions of calcined samples	S_{BET} , m ² /g
	Cu	Zn	Si	Cr	Al			
Cu–Si	14	0	86	0	0	450	Cu hydrosilicate with <i>chrysocolla</i> -type structure + SiO ₂	300
Cu–Zn–Si	15	30	55	0	0	450	Cu–Zn silicate of the zincsilite type	250
Cu–Al–Zn	30	60	0	0	10	350	Solid solution of Cu,Al in a.m. ZnO with wurtzite structure	120
CuCr ₂ O ₄	33	0	0	67	0	900	Cu chromite with the spinel structure	80

Table 2. Phase composition of the samples after activation in hydrogen, Cu⁰ particle size, and specific surface areas of Cu⁰

Sample	Temperature of activation in H ₂ , °C	Phase composition after activation*	Cu ⁰ particle size, nm	Specific surface area of Cu ⁰ , m ² /g _{cat}
Cu–Si	450	Cu ⁰ /SiO ₂	3–6	31
Cu–Zn–Si	380	Cu ⁰ /ZS	3–4	8
Cu–Al–Zn	270	Cu ⁰ //ZnO	3–5	9
CuCr ₂ O ₄	300	Cu ⁰ //spinel	3–10	6

*// is epitaxially bonded.

- Cu–Al–Zn oxide model catalyst based on anionically modified (a.m.) ZnO (an analog of the industrial catalyst of methanol synthesis);

- copper chromite with spinel structure (CuCr₂O₄).

The aim of this work is to determine the conditions for conducting the methanol dehydrogenation process with high selectivity toward either methyl formate or syngas.

EXPERIMENTAL

Preparation of samples. Samples of copper-containing oxide catalysts were produced via the thermal treatment of combined hydrocompound precursors at the optimum temperatures presented in Table 1 for each composition (350–900°C). Hydrocompounds Cu–Si and Cu–Zn–Si were obtained via deposition–precipitation under conditions of urea hydrolysis (DPU) using the procedure described in [14]. Cu–Al–Zn and CuCr₂O₄ were obtained via coprecipitation [15], ensuring the deep chemical interaction of components. The chemical and phase compositions of the samples are presented in Table 1.

All of the investigated catalysts were reduced in hydrogen at the optimum temperatures for each sample (260–380°C) prior to testing their catalytic properties (Table 2).

The specific surface area of metallic copper was measured via pulse titration of N₂O with chromatographic analysis [16]. Using the results in [17], the surface was calculated from the amount of fast reacting

N₂O in order to eliminate the effect of bulk Cu⁰ oxidation. The specific surface area of metallic copper was calculated by assuming there was one oxygen atom per every two surface metallic copper atoms, and the surface density of the copper atoms was 1.6×10^{19} at/m² (the average value from Cu planes Cu (100), (110), and (111)) [18]. The values of specific surface area of Cu⁰ are presented in Table 2.

Catalytic measurements were performed in a laboratory-scale fixed-bed reactor at atmospheric pressure and a temperature of 200°C using gas chromatography to analyze the composition of the reaction mixture. The initial gas reaction mixture was approximately 16 vol % of methanol in helium. A detailed description of the procedure used for catalytic measurements and processing of results was given in [19].

RESULTS AND DISCUSSION

Sample Characteristics

The chemical and phase compositions determined from the XRD data, and the total specific surface area determined from the BET data of the calcined samples, are presented in Table 1. The obtained samples were single-phase, allowing us to obtain clear catalytic characteristics in the reaction of methanol dehydrogenation.

The phase compositions of the samples following reduction in hydrogen are presented in Table 2. It can be seen from the XRD and HRTEM data that certain changes occurred in the composition of the samples

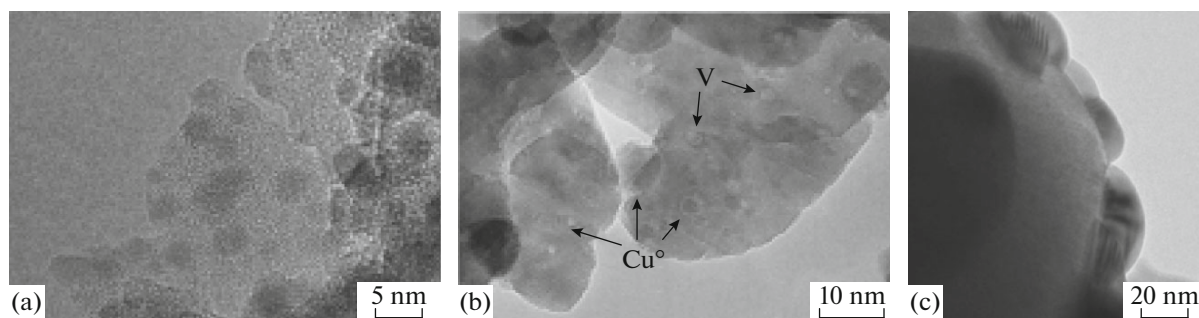


Fig. 1. Microphotographs of the reduced samples (a) Cu–Zn–Si (380°C) [21], (b) Cu–Al–Zn (270°C) [15], (c) CuCr₂O₄ (300°C) in a dark field [22].

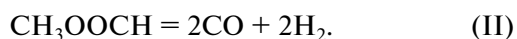
during reduction: The copper hydrosilicate with chrysocolla-type structure was converted into amorphous silica with Cu⁰ nanoparticles 3–6 nm in size distributed over its surface; the copper–zinc hydrosilicate with the zincsilite (ZS) structure retained it with Cu⁰ nanoparticles 3–4 nm in size distributed over its surface [20, 21]; the Cu–Al–Zn catalyst, a solid solution of copper and aluminum ions in zinc oxide with wurtzite structure (ZnO), retained it with flat epitaxially bonded Cu⁰ nanoparticles distributed over its surface [15]; and copper chromite retained its spinel-type structure with Cu⁰ particles 3–10 nm in size distributed over the oxide's surface [22, 23].

Microphotographs of the reduced Cu–Zn–Si, Cu–Al–Zn, and CuCr₂O₄ samples are presented in Fig. 1. The microphotograph of Cu–Si is not presented, since the sample decomposed when subjected to the electron beam.

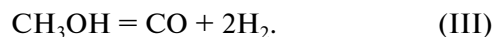
The Cu⁰ nanoparticles in the samples of different compositions differ only slightly in size (3–10 nm; see Table 2), but they differ greatly in morphology. Investigation of the samples by various physicochemical methods including HRTEM (see Fig. 1) showed that the Cu⁰ nanoparticles interacted differently with the oxide support: in the Cu–Al–Zn and CuCr₂O₄ samples, the Cu⁰ nanoparticles were epitaxially bonded to the surfaces of ZnO and spinel, respectively [22, 24]. No such bond formed with Cu–Si and Cu–Zn–Si. On the other hand, the decoration of Cu⁰ nanoparticles with clusters of their supporting material has been mentioned in the literature [25, 26].

Catalytic Properties

It was shown in [12, 13] that methanol dehydrogenation over copper-containing catalysts proceeds according to the sequential scheme



The sum of these reactions comprises the process of methanol decomposition into syngas:



This is why the catalytic properties of the catalysts were assessed by comparing the values of their specific activities in the reaction of methanol conversion with the formation of methyl formate according to reaction path (I), and of CO according to reaction path (I + II). The specific activities were presented as rates of the formation of a specified product, normalized with respect to the specific surface area of the metallic copper.

Methanol decomposition to syngas (III) is virtually unlimited thermodynamically: $K_p^{\text{III}}(200^\circ\text{C}) = 6.8 \times 10^2$, which corresponds to an equilibrium methanol conversion of more than 99.9% under test conditions. With the kinetic hindrance of reaction (II), however, methanol conversion is limited by the partial equilibrium of reaction (I).

The theoretical dependences of the selectivity of methyl formate formation on the methanol conversion at 200°C and initial partial methanol pressures of 0.16, 1, and 5 atm under conditions of partial equilibrium according to reaction (I) are presented in Fig. 2. Selectivity (S) and the methanol conversion (X) are determined by Eqs. (1) and (2) for a mixture of methanol and helium (initial partial pressures of 0.16 atm for methanol and 0.84 atm for helium) and a constant reaction mixture pressure of 1 atm:

$$K_{p1} = \frac{(\xi_1 - \xi_2)4(\xi_1 + \xi_2)^2}{(n_1^0 - 2\xi_1)^2(6.25n_1^0 + \xi_1 + 3\xi_2)} \left(\frac{P}{P_0}\right) \quad (1)$$

$$= 3.4 \times 10^{-2},$$

$$S = \frac{\xi_1 - \xi_2}{\xi_1}; \quad X = \frac{2\xi_1}{n_1^0}, \quad (2)$$

where ξ_1 and ξ_2 are chemical variables of reactions (I) and (II), respectively, moles; n_1^0 is the initial amount of methanol in the reaction mixture, moles; $P = 1$ atm is the pressure in the reactor, $P_0 = 1$ bar (standard pressure). The equilibrium constant of reaction (I) is assumed to be 3.4×10^{-2} for purposes of calculation [27].

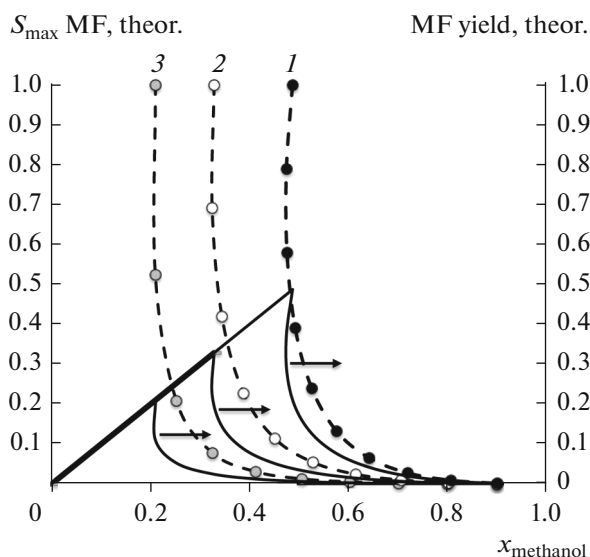


Fig. 2. Maximum theoretical selectivity (dot-and-dash lines) and methyl formate yield (solid lines) at 200°C, constant pressure, and initial partial pressures (1) $P_{\text{MeOH}} = 0.16$ atm, $P_{\text{He}} = 0.84$ atm, (2) $P_{\text{MeOH}} = 1$ atm, (3) $P_{\text{MeOH}} = 5$ atm.

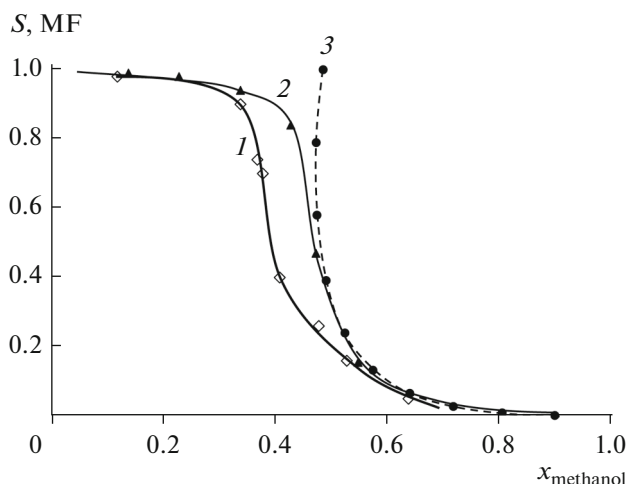


Fig. 3. Experimental dependences of selectivity for methyl formate (S , MF) on the methanol conversion (X) at 200°C: (1) Cu-Si, (2) Cu-Zn-Si, (3) calculated equilibrium curve of partial pressure for reaction (I) at a partial methanol pressure of 0.16 atm.

The obtained dependences show a complex pattern: The selectivity for methyl formate can be as high as 100% up to a methanol conversion of approximately 48.8% at the initial partial pressure of methanol of 0.16 atm. Points $X = 48.8\%$ and $S = 100\%$ correspond to the equilibrium conditions of reaction (I) with no occurrence of reaction (II). The increase in chemical variable ξ_2 that obviously represents a decrease in process selectivity first results in a slight reduction of the equilibrium methanol conversion (due to the release of

hydrogen in reaction (II)). At high ξ_2 values, it raises the methanol conversion to more than 98%. The partial equilibrium curve in coordinates $S(X)$ is bifurcated in the range of $X = 47\text{--}49\%$. In practice, this translates into a large, sharp drop in selectivity for methyl formate, with a slight increase in the methanol conversion.

The maximum theoretical yield of methyl formate (see Fig. 2) at very brief contact times thus changes in proportion to the methanol conversion. The theoretical yield of methyl formate reaches its maximum level of 0.488 under conditions of an initial partial methanol pressure of 0.16 atm in the mixture with helium, followed by a sharp drop. The increased pressure negatively affects the equilibrium in reaction (I) and reduces the maximum theoretical yield of MF. For example, the theoretical yield of MF at a methanol pressure of 1 atm is only 0.329.

The real selectivity of methyl formate formation during methanol dehydrogenation is lower than the theoretical one, but it also depends strongly on the methanol conversion (Fig. 3). At brief contact times, the methanol consumption of all our catalysts is accompanied by the accumulation of methyl formate, and no formation of CO is observed in the process. The selectivity of methyl formate formation is therefore close to 100%. The yield of methyl formate grows along with the contact time, reaches its maximum, and then falls to a relatively low value. The contact time at which CO formation becomes noticeable varies for different catalysts, and the CO yield grows along with the contact time. This dependence has an inflection point at the maximum of methyl formate concentration [19]. These observations, along with the results from other kinetic experiments described in [12, 13], indicate that the dehydrogenation of methanol to CO and hydrogen proceeds via the formation of intermediate methyl formate according to the scheme of sequential reactions (I) and (II). The selectivity of the catalyst based on the copper-zinc hydrosilicate Cu-Zn-Si activated at 380°C approaches the maximum theoretical selectivity of the process (see Fig. 3).

The proximity of the real dependence of selectivity (and thus the yield of methyl formate) to the partial pressure curve is due to the ratio of the W_I/W_{II} rates of reactions (I) and (II) and depends on the properties of the catalyst that was used. The values of these rates, normalized with respect to the catalyst mass and the units of the surface area of metallic copper at a temperature of 200°C, are presented in Table 3. The reaction rates were determined using the initial partial methanol pressure $P_{\text{MeOH}} = 0.16$ atm. Methyl formate was initially present in the mixture with helium ($P_{\text{MF}} = 0.018$ atm) when determining the rate of CO formation. It can be seen that the investigated copper-containing catalysts display different W_I/W_{II} ratios.

The high selectivity of methanol dehydrogenation toward methyl formate is due to our selection of an efficient catalyst and the conditions of the process

Table 3. Rates of methanol and methyl formate dehydrogenation reactions at 200°C and initial partial methanol pressure $P_{\text{MeOH}} = 0.16$ atm

Parameter	Catalyst sample			
	Cu–Si	Cu–Zn–Si	Cu–Al–Zn	CuCr ₂ O ₄
W_{I} , molecules/(g s)	6.0×10^{19}	6.6×10^{18}	3.8×10^{17}	15.4×10^{18}
W_{II} , molecules/(g s)	1.3×10^{19}	1.6×10^{17}	1.6×10^{16}	8.0×10^{17}
W_{I}^* , molecules/(m ² s)	19.4×10^{17}	9.4×10^{17}	4.8×10^{16}	2.6×10^{18}
W_{II}^* , molecules/(m ² s)	4.2×10^{17}	2.3×10^{16}	2.0×10^{15}	1.3×10^{17}
$W_{\text{I}}/W_{\text{II}}$	≈ 4.6	≈ 40.8	≈ 24	≈ 19.2

Table 4. Productivity of methyl formate (MF) at 200°C and an initial partial methanol pressure of $P_{\text{MeOH}} = 0.16$ atm

Sample	T_{cont} , s	X , %	S , %	Productivity g _{MF} /(g _{cat} h)
Cu–Al–Zn	0.3	20	90	1.7
Cu–Zn–Si	0.5	26	95	0.69
	0.05*	32*	95*	3.3*
CuCr ₂ O ₄	0.05	30	95	2.1
CuMgSi** [27]	0.6	14	83	0.66

* At 300°C.

** Reaction was conducted in pure methanol, $P_{\text{MeOH}} = 1$ atm.

(temperature and contact time). Of all the investigated catalysts, copper nanoparticles, produced via the reduction of copper hydrosilicate, are the least selective, since they display maximum activity in the reaction (II) of CO formation. This catalyst is therefore an effective one for the production of syngas from methanol. Estimates based on laboratory testing show that the productivity of the Cu–Si catalyst for syngas is as high as $20 \text{ m}^3_{\text{STP}}/(\text{g}_{\text{cat}} \text{ h})$ at an initial partial methanol pressure of 1 atm, a temperature of 200°C, and a contact time of 0.5 s.

At the same time, the copper nanoparticles produced via reduction from the copper–zinc hydrosilicate, from copper chromite, and from the a.m. solid solution of copper–zinc–aluminum oxides with wurtzite structure can form the basis of a catalyst for the direct production of CO-free methyl formate from methanol. A comparative estimate of the productivities of methyl formate under our experimental conditions is presented in Table 4. Note that the methanol conversion of 14% reached in testing the CuMgSi catalyst recommended for methyl formate production in [28] is far from the conditions of partial equilibrium of reaction (I). The higher pressure of methanol used in testing this catalyst can therefore only accelerate the rate of methanol conversion. At the same time, the catalysts based on copper–zinc silite, the combined oxide of copper–aluminum–zinc with wurtzite struc-

ture, and the copper chromite are more active than the abovementioned CuMgSi catalyst, and more selective.

It follows from the results obtained in [2–6, 8, 10, 11] that even though metallic copper nanoparticles are an active component of all of the investigated catalysts based on copper and copper–zinc hydrosilicates, along with the samples of copper–zinc–aluminum and copper–chromium oxides, the specific activities of these catalysts differ substantially, either with respect to methyl formate formation or its decomposition. In other words, the catalytic properties of the investigated samples depend on the composition and structure of the catalyst precursor compounds:

(1) In the region of low methanol conversions, the process of methanol dehydrogenation is essentially represented by reaction (I), which proceeds far from its equilibrium.

(2) In the region of high methanol conversions, reaction (I) is close to equilibrium, and the rate of the total process is determined by reaction (II).

(3) In the region of moderate methanol conversions up to those corresponding to the partial equilibrium of reaction (I), the process is determined by the ratio of the rates of the sequential reactions, and the methyl formate content depends on the catalyst's composition.

It is in region (3) where the sensitivity to the nature of the precursor compound is most pronounced. The

higher the W_I/W_{II} ratio, the closer the real selectivity and the yield of methyl formate are to the theoretical maxima. The highest yield of methyl formate is thus obtained over the catalyst based on the copper–zinc hydrosilicate Cu–Zn–Si. This catalyst was activated at 380°C and operated stably for 340 h as the temperature rose from 160 to 260°C. Its activity was nearly halved after the first 100 h at 160°C; it then grew according to the temperature dependence of the rate constant and remained at the same level at 260°C for 50 h.

CONCLUSIONS

Our investigation of the catalytic properties of CuZnAl and Cu–Zn–Si oxide catalysts, performed for a wide range of contact times, and our analysis of thermodynamics of the process of methanol dehydrogenation, allowed us to determine the dependences of process selectivity and the methyl formate yield on the process conditions and the nature of the catalyst:

(1) It was confirmed that the reaction of methanol dehydrogenation proceeds sequentially with the formation of methyl formate as an intermediate compound according to reactions (I) and (II).

The selectivity of the process and the yield of methyl formate are determined by both the activity and selectivity of the investigated catalysts in reactions (I) and (II), and by the thermodynamics of the process. The thermodynamic limitations are apparent in the strong dependence of the process's selectivity on the methanol conversion.

In the region of low methanol conversions, the combined dehydrogenation process is mainly represented by reaction (I), which proceeds far from its equilibrium.

In the region of high methanol conversions, reaction (I) is close to the partial equilibrium, and the reaction rate of the total process is determined by reaction (II).

In the region of moderate methanol conversions, the dependence of the maximum theoretical selectivity of the process on the conversion is bifurcated. A sharp decrease in selectivity as the contact time grows characterizes the real process in this region. The proximity of reaction (I) to partial equilibrium and the maximum theoretical selectivity is determined by the ratio of the rates of two sequential reactions (the higher the W_I/W_{II} ratio, the closer the process is to the partial equilibrium of reaction (I)), and the yield of methyl formate depends on the catalyst's composition.

The region of the methanol conversion where a sharp drop in the selectivity toward methyl formate is observed shifts toward lower values with an increase in pressure: the theoretical yield of methyl formate can be as high as 48% at a pressure of 0.16 atm, while increasing the pressure to 5 atm reduces the maximum theoretical yield of methyl formate to 21%. It is therefore

advisable to conduct the process at the lowest possible pressure.

(2) In both in the reaction of methyl formate formation and the reaction of its dehydrogenation, the activity is determined by the nanoparticles of metallic copper formed as a result of catalyst reduction, and depends on the composition and structure of the precursor of the catalyst. The catalysts based on Cu–zinc–silite, copper chromite, and a.m. solid solutions of Cu and Al in ZnO with wurtzite structure demonstrate high activity in reaction (I) and only moderate activity in reaction (II). They can be used for the direct production of methyl formate from methanol with high selectivities of more than 90%. The catalyst based on Cu–zinc–silite allows us to conduct the process with more than 95% selectivity toward methyl formate. The catalyst based on copper hydrosilicate of the chrysocolla type exhibits high activity in the reaction of methyl formate dehydrogenation (II) and is an effective catalyst for decomposition of methanol into syngas.

ACKNOWLEDGMENTS

This work was supported by the Russian Academy of Sciences, the Federal Agency of Scientific Organizations of Russia (project no. V.45.3.6); and the Novosibirsk State University (scientific project no. 2211, a part of state task no. 2014/139). The authors are grateful to M.P. Demeshkina for preparing our catalyst samples.

REFERENCES

1. Lee, J.S., Kim, J.C., and Kim, Y.G., *Appl. Catal., A*, 1990, vol. 57, no. 1, pp. 1–30.
2. Sodesawa, T., *React. Kinet. Catal. Lett.*, 1986, vol. 32, no. 1, pp. 51–56.
3. Sodesawa, T., Nagacho, M., Onodera, A., and Nozaki, F., *J. Catal.*, 1986, vol. 102, no. 2, pp. 460–463.
4. Guerreiro, E.D., Gorrioz, O.F., Rivarola, L.A., and Arrúa, L.A., *Appl. Catal., A*, 1997, vol. 165, nos. 1–2, pp. 259–271.
5. Guerreiro, E.D., Gorrioz, O.F., Larsen, G., and Arrúa, L.A., *Appl. Catal., A*, 2000, vol. 204, no. 1, pp. 33–48.
6. Galloa, Al., Tsoncheva, T., Marelli, M., Mihaylov, M., Dimitrov, M., Dal Santo, V., and Hadjiivanov, K., *Appl. Catal., B*, 2012, vol. 126, pp. 161–171.
7. Rodriguez-Ramos, I., Guerrero-Ruiz, A., Rojas, M.L., and Fierro, J.L.G., *Appl. Catal.*, 1991, vol. 68, no. 1, pp. 217–228.
8. Chung, M.-J., Moon, D.-J., Park, K.-Y., and Ihm, S.-K., *J. Catal.*, 1992, vol. 136, no. 2, pp. 609–612.
9. Lapidus, A.L., Antonyuk, S.N., Kapkin, V.D., Bruk, I.A., Sominskii, S.D., and Pechuro, N.S., *Neftekhimiya*, 1985, vol. 25, no. 6, pp. 761–765.
10. Wang, Y., Ruan, G. and Han, S., *React. Kinet. Catal. Lett.*, 1999, vol. 67, no. 2, pp. 305–310.

11. Sato, S., Iijima, M., Nakayama, T., Sodesawa, T., and Nozaki, F., *J. Catal.*, 1997, vol. 169, no. 2, pp. 447–454.
12. Shlegel', L., Gutshik, D., and Rozovskii, A.Ya., *Kinet. Katal.*, 1990, vol. 4, no. 4, p. 1000.
13. Gorshkov, S.V., Lin, G.I., and Rozovskii, A.Ya., *Kinet. Katal.*, 1999, vol. 40, no. 3, p. 372.
14. Yurieva, T.M., Kustova, G.N., Minyukova, T.P., Poels, E.K., Blik, A., Demeshkina, M.P., Plyasova, L.M., Krieger, T.A., and Zaikovskii, V.I., *Mater. Res. Innovations*, 2001, vol. 5, no. 1, pp. 3–11.
15. Yurieva, T.M., Plyasova, L.M., Zaikovskii, V.I., Minyukova, T.P., Blik, A., Heuvel, J.C., Davydova, L.P., Molina, I.Yu., Demeshkina, M.P., Khassin, A.A., and Batyrev, E.D., *Phys. Chem. Chem. Phys.*, 2004, vol. 6, no. 18, pp. 4522–4526.
16. Scholten, J.J.F. and Konvalinka, J.A., *Trans. Faraday Soc.*, 1969, vol. 65, pp. 2465–2473.
17. Sato, S., Takahashi, R., Sodesawa, T., Yuma, K.-I., and Obata, Y., *J. Catal.*, 2000, vol. 196, no. 1, pp. 195–199.
18. Evans, J.W., Wainwright, M.S., Bridgewater, A.J., and Young, D.J., *Appl. Catal.*, 1983, vol. 7, no. 1, pp. 75–83.
19. Minyukova, T.P., Simentsova, I.I., Khasin, A.V., Shtertser, N.V., Baronskaya, N.A., Khassin, A.A., and Yurieva, T.M., *Appl. Catal., A*, 2002, vol. 237, nos. 1–2, pp. 171–180.
20. Yurieva, T.M., Minyukova, T.P., Kustova, G.N., Plyasova, L.M., Krieger, T.A., Demeshkina, M.P., Zaikovskii, V.I., Malakhov, V.V., and Dovlitova, L.S., *Mater. Res. Innovations*, 2001, vol. 5, no. 2, pp. 74–80.
21. Minyukova, T.P., Shtertser, N.V., Khassin, A.A., Plyasova, L.M., Kustova, G.N., Zaikovskii, V.I., Shvedenkov, Yu.G., Baronskaya, N.A., van den Heuvel, J.C., Kuznetsova, A.V., Davydova, L.P., and Yurieva, T.M., *Kinet. Catal.*, 2008, vol. 49, no. 6, pp. 821–830.
22. Makarova, O.V., Yurieva, T.M., Kustova, G.N., Ziborov, A.V., Plyasova, L.M., Minyukova, T.P., and Zaikovskii, V.I., *Kinet. Catal.*, 1993, vol. 34, no. 4, pp. 608–612.
23. Khassin, A.A., Kustova, G.N., Jobic, H., Yurieva, T.M., Chesalov, Yu.A., Filonenko, G.A., Plyasova, L.M., and Parmon, V.N., *Phys. Chem. Chem. Phys.*, 2009, vol. 11, no. 29, pp. 6090–6097.
24. Yurieva, T.M., *Catal. Today*, 1999, vol. 51, nos. 3–4, pp. 457–467.
25. Vitonen, M.M., Jansen, W.P.A., van Welzenis, R.G., Brongerma, H.H., Brands, D.S., Poels, E.K., and Blik, A., *J. Phys. Chem. B*, 1999, vol. 103, no. 29, pp. 6025–6029.
26. Zhang, Z., Patterson, M., Ren, M., Wang, Y., Flake, J.C., Sprunger, P.T., and Kurtz, R.L., *J. Vac. Sci. Technol., A*, 2013, vol. 31, no. 1, p. 01A144.
27. Stull, D.R., Westrum, E.F., and Sinke, G.C., *The Chemical Thermodynamics of Organic Compounds*, New-York: John Wiley and Sons, 1969.
28. US Patent 5194675, 1993.

Translated by L. Brovko